Performance—Complexity Comparison of Receivers for a LTE MIMO–OFDM System

Johanna Ketonen, *Student Member, IEEE*, Markku Juntti, *Senior Member, IEEE*, and Joseph R. Cavallaro, *Senior Member, IEEE*

***Abstract*—Implementation of receivers for spatial multiplexing multiple-input multiple-output (MIMO) orthogonal-frequency-division-multiplexing (OFDM) systems is considered. The linear minimum mean-square error (LMMSE) and the K-best list sphere detector (LSD) are compared to the iterative successive interference cancellation (SIC) detector and the iterative K-best LSD. The performance of the algorithms is evaluated in 3G long-term evolution (LTE) system. The SIC algorithm is found to perform worse than the K-best LSD when the MIMO channels are highly correlated, while the performance difference diminishes when the correlation decreases. The receivers are designed for 2×2 and 4×4 antenna systems and three different modulation schemes. Complexity results for FPGA and ASIC implementations are found. A modification to the K-best LSD which increases its detection rate is introduced. The ASIC receivers are designed to meet the decoding throughput requirements in LTE and the K-best LSD is found to be the most complex receiver although it gives the best reliable data transmission throughput. The SIC receiver has the best performance–complexity tradeoff in the 2×2 system but in the 4×4 case, the K-best LSD is the most efficient. A receiver architecture which could be reconfigured to using a simple or a more complex detector as the channel conditions change would achieve the best performance while consuming the least amount of power in the receiver.**

***Index Terms*—ASIC, FPGA, K-best, SIC, soft-output detector.**

I. Introduction

MULTIPLE-INPUT multiple-output (MIMO) systems offer an increase in capacity or diversity. Herein we focus on the data transmission rate increase provided by spatial multiplexing (SM). Orthogonal-frequency-division multiplexing (OFDM) is a popular technique for wireless high data rate transmission, because it enables efficient use of the available bandwidth and a simple implementation. It divides the frequency selective fading channel into parallel flat fading subchannels. The combination of MIMO and OFDM is a promising wireless access scheme [1]. Timely examples of MIMO–OFDM applications include the evolving third-generation (3G) cellular systems known as long-term evolution (LTE) and worldwide interoperability for microwave access (WiMAX) system.

Transmission of independent data streams from different antennae in SM–MIMO systems usually causes spatial multiplexing interference (SMI) or inter-antenna interference. This calls for sophisticated receiver designs to cope with the interference. The optimal detector would be the maximum *a posteriori* probability (MAP) symbol detector providing soft outputs or log-likelihood ratio (LLR) values to the forward error control (FEC) decoder. Since the computational complexity of both MAP and maximum likelihood (ML) detectors depends exponentially on the number of spatial channels and modulation symbol levels, several suboptimal solutions have been proposed and studied.

Linear minimum mean-square error (LMMSE) or zero-forcing (ZF) detection principles can be straightforwardly applied in MIMO detection. However, the linear detectors can suffer a significant performance loss in fading channels, in particular with spatial correlation between the antenna elements [2]. Ordered serial interference cancellation (OSIC) was proposed already in the original papers considering the Bell Laboratories layered space-time (BLAST) architecture [3]–[5]. Therein, instead of jointly detecting signals from all the antennas, the strongest signal can be detected first and its interference can be cancelled from each received signal. In FEC encoded systems, the detected symbols are decoded before cancellation. The soft bit decisions from the turbo decoder are used to calculate symbol expectations which are cancelled from the remaining layers [6], [7].

Sphere detectors (SDs) calculate the ML solution by taking into account only the lattice points that are inside a sphere of a given radius [8], [9]. A list sphere detector (LSD) approximates the MAP detector and provides soft outputs for the FEC decoder [10]. The breadth-first tree search based K-best LSD algorithm is a modification of the K-best algorithm [11], [12]. The depth-first [13] and metric-first [14] sphere detectors have a closer to optimal search strategy and achieve a lower bit error rate than the breadth-first detector. However, the K-best LSD is considered in this paper because it can be easily pipelined and parallelized and provides a fixed detection rate. The breadth-first K-best LSD can also be more easily implemented and provide the high and constant detection rates required in the LTE.

Sphere detector implementations for mostly a 4×4 antenna system and 16-quadrature amplitude modulation (QAM) have

Manuscript received October 15, 2009; accepted January 31, 2010. Date of publication February 25, 2010; date of current version May 14, 2010. The associate editor coordinating the review of this manuscript and approving it for publication was Prof. Jarmo Takala. This research has been supported in part by Elektrobit, Nokia, Nokia Siemens Networks, Texas Instruments, Uninord, the Finnish Funding Agency for Technology and Innovation (TEKES), Xilinx and by the US National Science Foundation under Grants CCF-0541363, CNS-0551692, CNS-0619767, EECS-0925942, and CNS-0923479. This paper was presented in part at the Annual Asilomar Conference on Signals, Systems, and Computers, Pacific Grove, CA, October 2008.

J. Ketonen and M. Juntti are with the Centre for Wireless Communications, University of Oulu, Oulu FIN-90014, Finland (e-mail: (johanna.ketonen@ee.oulu.fi; markku.juntti@ee.oulu.fi)

J. R. Cavallaro is with the Department of Electrical and Computer Engineering, Rice University, Houston, TX 77005 USA (e-mail: cavallar@rice.edu).

Color versions of one or more of the figures in this paper are available online at http://ieeexplore.ieee.org.

Digital Object Identifier 10.1109/TSP.2010.2044290

been reported in the literature. Application-specific integrated circuit (ASIC) implementation of a soft output K-best sphere decoding algorithm has been presented in [12], a fixed sphere decoder in [15] and optimizations of a hard-output K-best in [16]. An application-specific instruction set processor (ASIP) has been designed for a 2×2 64-QAM system K-best LSD with transport triggered architecture (TTA) in [17]. An FPGA implementation of a hard output breadth-first sphere detector can be found in [18]. ASIC implementations of depth-first and K-best sphere decoding algorithms have been presented in [19].

We compared the SIC and K-best LSD implementations for a field-programmable gate array (FPGA) in [20]. The receivers were designed for 2×2 4-QAM, 16-QAM, and 64-QAM and implemented with the Xilinx System Generator. The SIC receiver was found to be slightly more complex than the K-best LSD receiver, but the latency of the SIC receiver was lower with all modulations. However, a complete analysis of the achievable communication performance and required implementation complexity with various detectors in the evolving LTE standard has received very little if any attention in the open literature.

In this paper, we analyze the performance–complexity tradeoff of various soft-output MIMO detectors in the LTE system downlink context. More specifically, the performances, implementation complexities and latencies of the plain LMMSE, the LMMSE based SIC receiver and the K-best LSD receiver are studied and compared to each other; a modification to the tree search of the K-best LSD is also introduced to simplify its implementation. FPGA and ASIC implementation results are presented for 2×2 and 4×4 MIMO configurations with QPSK, 16-QAM, and 64-QAM. Their communication system performances are compared via computer simulations with LTE parameters [21] and realistic channel models. The latency of the entire receiver is considered and the iterative (turbo) versions of the SIC and K-best LSD are compared to the noniterative LMMSE and K-best LSD receivers.

The results provide a solid basis for systematic complexity-performance tradeoff of different detection algorithms for application in the evolving next generation cellular access standard. The communication system performance is characterized by frame error rate (FER), which is usually transformed to data *transmission throughput*. The transmission throughput is defined to be equal to the nominal information transmission rate of information bits times $(1 - \mathrm{FER})$. In other words, the throughput measure characterizes the rate and the reliability. The implementation complexity is characterized as the numbers of FPGA slices, 18-kbit blocks of random access memory (BRAM) and dedicated digital signal processor (DSP) slices as well as equivalent gates. The latency of the implementation is also analyzed, and reflected as *detection rate* of a particular implementation. The detection rate refers to the nominal rate by which the algorithm can make data decisions, but it differs from the transmission throughput in the sense that it tells nothing about the reliability of the decisions. The measure which combines both the hardware limitations and the reliability is called *goodput*, i.e., the minimum of the transmission throughput and hardware detection rate of information bits.

The paper is organized as follows. The system model is presented in Section II-A. The K-best LSD algorithm is introduced in Section II-B. The SIC algorithm is introduced in Section II-C. Some performance examples are presented in Section III. The complexities and latencies are compared in Section IV. Discussion and conclusions are presented in Sections V and VI.

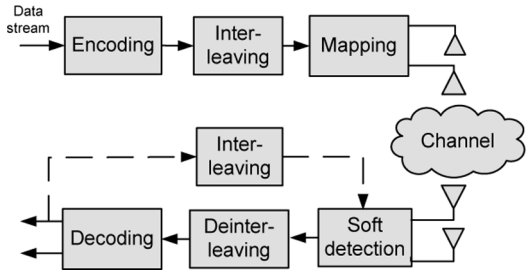

Fig. 1. The MIMO–OFDM system model.

II. Receiver Algorithms

A. System Model

An OFDM based MIMO transmission system with N transmit (TX) and M receive (RX) antennas, where $N \leq M$, is considered in this paper. A layered space-time architecture with horizontal encoding is applied. The cyclic prefix of an OFDM symbol is assumed to be long enough to eliminate intersymbol interference. The system model is illustrated in Fig. 1. The received signal can be described with the equation

$$\mathbf{y}_p = \mathbf{H}_p \mathbf{x}_p + \eta_p, \quad p = 1, 2, \ldots, P \tag{1}$$

where P is the number of subcarriers, $\mathbf{x}_p \in \mathbb{C}^N$ is the transmitted signal on pth subcarrier, $\eta_p \in \mathbb{C}^M$ is a vector containing identically distributed complex Gaussian noise with variance σ^2 and $\mathbf{H}_p \in \mathbb{C}^{M \times N}$ is the channel matrix containing complex Gaussian fading coefficients. Bit-interleaved coded modulation (BICM) is applied. The entries of $\mathbf{x}_p$ are drawn from a complex QAM constellation Ω and $|\Omega| = 2^Q$, where Q is the number of bits per symbol. The set of possible transmitted symbol vectors is Ω^N. The binary vector $\mathbf{b}_p$ corresponding to $\mathbf{x}_p$ has elements b^λ, where $\lambda = (k-1)Q, \ldots, kQ - 1$ with the kth element of $\mathbf{x}_p$.

B. The K-Best LSD Algorithm

The ML detection method minimizes the average error probability and it is the optimal method for finding the closest lattice point. The ML detector calculates the Euclidean distances (EDs) between the received signal vector $\mathbf{y}$ and lattice points $\mathbf{Hx}$, and returns the vector $\mathbf{x}$ with the smallest distance, i.e., it minimizes

$$\hat{\mathbf{x}}_{\mathrm{ML}} = \arg \min_{\boldsymbol{x} \in \Omega^N} \|\mathbf{y} - \mathbf{Hx}\|^2. \tag{2}$$

The SD algorithms solve the ML solution with a reduced number of considered candidate symbol vectors. They take into account only the lattice points that are inside a sphere of a given radius. The condition that the lattice point lies inside the sphere can be written as

$$\|\mathbf{y} - \mathbf{Hx}\|^2 \leq C_0. \tag{3}$$

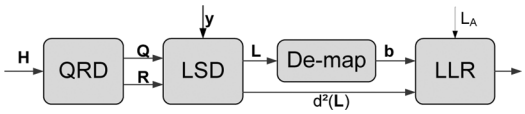

Fig. 2. The list sphere detector.

After QR decomposition (QRD) of the channel matrix $\mathbf{H}$ in (3), it can be rewritten as

$$\|\mathbf{y}' - \mathbf{R}\mathbf{x}\|^2 \leq C_0' \tag{4}$$

where $C_0' = C_0 - \|(\mathbf{Q}')^{\mathrm{H}}\mathbf{y}\|^2, \mathbf{y}' = \mathbf{Q}^{\mathrm{H}}\mathbf{y}$, $\mathbf{R} \in \mathbb{C}^{N\times N}$ is an upper triangular matrix with positive diagonal elements, $\mathbf{Q} \in \mathbb{C}^{M\times N}$ and $\mathbf{Q}' \in \mathbb{C}^{M\times(M-N)}$ are orthogonal matrices.

The squared partial Euclidean distance (PED) of $\mathbf{x}_i^N$, i.e., the square of the distance between the partial candidate symbol vector and the partial received vector, can be calculated as

$$d\left(\mathbf{x}_i^N\right) = \sum_{j=i}^{N}\left|y_j' - \sum_{l=j}^{N} r_{j,l}x_l\right|^2 \tag{5}$$

where $i = N\ldots,1$ and $\mathbf{x}_i^N$ denotes the last $N-i+1$ components of vector $\mathbf{x}$ [8].

LSD can be used to approximate the MAP detector and to provide soft outputs for the decoder [10]. A list of candidates $\mathcal{L}$ and their Euclidean distances are used to calculate the *a posteriori* probabilities of the coded bits in $\mathbf{b}_p$.

The K-best algorithm [11] is a breadth-first search based algorithm, which keeps the K nodes which have the smallest accumulated Euclidean distances at each level. If the PED is larger than the squared sphere radius C_0, the corresponding node will not be expanded. We assume no sphere constraint or $C_0 = \infty$, but set the value for K instead, as is common with the K-best algorithms.

A LSD structure is presented in Fig. 2. The channel matrix $\mathbf{H}$ is first decomposed as $\mathbf{H} = \mathbf{QR}$ in the QR-decomposition block. The Euclidean distances between the received signal vector $\mathbf{y}$ and the possible transmitted symbol vectors are calculated in the LSD block. The candidate symbol list $\mathcal{L}$ from the LSD block is demapped to a binary form.

The LLRs are calculated from the list of Euclidean distances in the LLR block. The log-likelihood ratio $L(x_k)$ for the transmitted bit k can be determined as

$$\begin{aligned} L(x_k) &= \ln\frac{\Pr(x_k = +1\,|\,\mathbf{y})}{\Pr(x_k = -1\,|\,\mathbf{y})} \\ &= \ln(p(\mathbf{y}\,|\,x_k = 1)) - \ln(p(\mathbf{y}\,|\,x_k = -1)). \end{aligned} \tag{6}$$

The approximation of $L(x_k)$ in (6) is calculated using a small lookup table and the Jacobian logarithm

$$\mathrm{jacln}(a_1,a_2) := \ln(e^{a_1}+e^{a_2}) = \max(a_1,a_2) + \ln(1+e^{-|a_1-a_2|}). \tag{7}$$

The Jacobian logarithm in (7) can be computed without the logarithm or exponential functions by storing $r(|a_1 - a_2|)$ in a lookup table, where $r(\cdot)$ is a refinement of the approximation $\max(a_1, a_2)$ [10]. Limiting the range of LLRs reduces the required list size K [22].

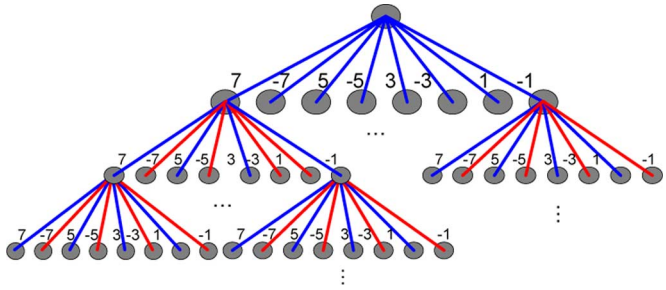

Fig. 3. The modified tree search.

The output of the turbo decoder can also be utilized in the LSD receiver. The LLRs on the first iteration are calculated also as previously presented. On the second iteration, the soft bit LLRs from the decoder are used to update the LLRs with

$$\begin{aligned} \hat{L}_D(b_k\,|\,\mathbf{y}) &= L_A(b_k) \\ &\quad + \ln\frac{\sum_{\mathbf{b}\in\mathcal{L}_{k,+1}}\exp(\Lambda(\mathbf{b},\mathbf{b}_{[k]},\mathbf{l}_{A,[k]}\,|\,\mathbf{y},\mathbf{H}))}{\sum_{\mathbf{b}\in\mathcal{L}_{k,-1}}\exp(\Lambda(\mathbf{b},\mathbf{b}_{[k]},\mathbf{l}_{A,[k]}\,|\,\mathbf{y},\mathbf{H}))} \end{aligned} \tag{8}$$

where

$$\left(\Lambda\left(\mathbf{b},\mathbf{b}_{[k]},\mathbf{l}_{A,[k]}|\mathbf{y},\mathbf{H}\right)\right) = -\frac{1}{2\sigma^2}\|\mathbf{y}-\mathbf{H}\mathbf{x}\|^2 + \frac{1}{2}\mathbf{b}_{[k]}^T\mathbf{l}_{A,[k]} \tag{9}$$

and $L_A(b_k)$ is *a priori* information from the decoder, $\mathbf{l}_{A,[k]}$ is a vector of L_A and $\mathbf{b}_{[k]}$ is a vector corresponding to k from $\mathbf{b}$ [23].

1) Enhanced Tree Search: The breadth-first tree search can be modified to decrease the latency. With our novel search strategy [24], two or more PEDs can be calculated in parallel and the largest ones are discarded. With 64-QAM, instead of having to sort 64 PEDs, there are only 32 PEDs to be sorted on each level when two PEDs are calculated in parallel. On the first level, the PEDs are calculated as with the original breadth-first search as shown in Fig. 3, where the nodes with red paths are discarded.

C. The SIC Algorithm

Instead of jointly detecting signals from all the antennas, the strongest signal is detected first and its interference is cancelled from each received signal in the SIC receiver. Then the second strongest signal is detected and cancelled from the remaining signals and so on. The detection method is called successive nulling and interference cancellation [4]. Due to the horizontal layering of the encoded streams in LTE, the detected layers can be decoded separately. Therefore, decoding can be performed only on the strongest layer first and on the remaining layers after interference cancellation.

The soft SIC receiver is illustrated in Fig. 4. The first layer is detected with the LMMSE detector. The LLR block calculates LLRs from the LMMSE equalizer outputs. The deinterleaved stream is decoded with a turbo decoder and symbol expectations are calculated. The expectations are cancelled from the second

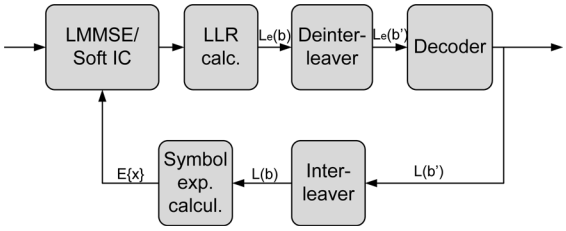

Fig. 4. The soft IC receiver.

layer, which is then decoded. The layer detected in the first iteration is not updated during the second iteration.

The weight matrix is calculated with the LMMSE algorithm

$$\mathbf{W} = (\mathbf{H}^{\mathrm{H}}\mathbf{H} + \sigma^2\mathbf{I}_M)^{-1}\mathbf{H}^{\mathrm{H}} \tag{10}$$

where $\mathbf{H}$ is the channel matrix, σ^2 is the noise variance, $(\cdot)^{\mathrm{H}}$ is the complex conjugate transpose and $\mathbf{I}_M$ is a $M \times M$ identity matrix. The layer for detection is chosen according to the post-detection SNR and the corresponding nulling vector is chosen from the weight matrix $\mathbf{W}$ [4]. All the weight matrices in an OFDM symbol are calculated and the layer to be detected is chosen according to the average over all the subcarriers.

After the first iteration, the cancelled symbol expectation is used to update the weight matrix. The weight matrix on the second iteration is calculated as

$$\begin{aligned}\mathbf{W} = &\left(E\{x\}E\{x\}^*\mathbf{h}_k\mathbf{h}_k^{\mathrm{H}}\right.\\ &\left.+\,\mathbf{H}_k\left(\mathbf{I} - (E\{x\}E\{x\}^*)\mathbf{H}_k^{\mathrm{H}} + \sigma^2\mathbf{I}_M\right)\right)^{-1}\mathbf{h}_k^{\mathrm{H}}\end{aligned} \tag{11}$$

where $\mathbf{h}_k$ is the kth vector from matrix $\mathbf{H}$, k is the layer to be detected, $\mathbf{H}_k$ is matrix $\mathbf{H}$ with the vectors from previously detected layers removed and $E\{x\}$ is the symbol expectation.

The LLRs can be calculated from the LMMSE equalizer outputs $\mathbf{z}$ as presented in [25] by using an approximate log-likelihood criterion. Instead of calculating the Euclidean distance between the LMMSE equalizer output and the possible transmitted symbols, Gray labeling of the signal points is exploited. This reduces the latency and complexity but was shown to have a minor impact on the performance. The bit-metric approximations $\hat{L}(b^\lambda|\mathbf{z},\mathbf{W})$ in [25] are calculated as

$$\rho_k\Lambda(b^\lambda,\mathbf{z}) = \min_{\tilde{x}_k\in\mathcal{X}^0_{k,\lambda}}|z_k - \tilde{x}_k|^2 - \min_{\tilde{x}_k\in\mathcal{X}^1_{k,\lambda}}|z_k - \tilde{x}_k|^2 \tag{12}$$

where $k = \lfloor\lambda/Q\rfloor + 1$, $\mathcal{X} = \{x_k : b^\lambda = i\}$ is the subset of hypersymbols $\{x\}$ for which the λth bit of label b is i and ρ_k is the signal-to-interference-and-noise ratio (SINR) of layer k. $\Lambda(b^\lambda,\mathbf{z})$ can be simplified by considering z_k in only one quadrature dimension given by λ.

The detected layer is decoded and symbol expectations from the soft decoder outputs are calculated as [26]

$$E\{x\} = \left(\frac{1}{2}\right)^Q\sum_{x_l\in\Omega}x_l\prod_{i=1}^{Q}(1 + b_{i,l}\tanh(L_A(b_i)/2)) \tag{13}$$

TABLE I
SIMULATION PARAMETERS

Coding	Turbo coding with 1/2 code rate
Channel model	TU, Uncorrelated
User Velocity	120 km/h
Number of subcarriers	512 (300 used)
Bandwidth	5 MHz
Symbol duration	71.4 μs

TABLE II
CHANNEL MODEL PARAMETERS

Number of paths	6
Path delays	[0...5000] ns
Path power	[−3...−10] dB
BS antenna spacing	4 λ
MS antenna spacing	0.5 λ
BS average angle of departure	50 °
MS average angle of arrival	67.5 °
BS azimuth spread	2 ° / 5 °
MS azimuth spread	35 °

where $L_A(b_i)$ are the LLRs of coded bits corresponding to x and $b_{i,l}$ are bits corresponding to constellation point x_l. The expectation calculation in (13) can be simplified to the form

$$E\{x\}_{\mathrm{re}} = \mathrm{sgn}(L_A(b_i))S|\tanh(L_A(b_{i+2}))|. \tag{14}$$

The constellation point S is chosen from $\{1,3,5,7\}$ depending on the signs of $L_A(b_{i+1})$ and $L_A(b_{i+2})$.

III. PERFORMANCE COMPARISONS

The communication system, i.e., the transmission throughput performance of the SIC detector is compared to that of the K-best LSD and the LMMSE detectors. The simulation parameters are based on the LTE standard [21] and are summarized in Table I. In the horizontally encoded LTE system, two data streams are encoded separately and then mapped onto different layers. The strongest layer can be detected and decoded first and then cancelled from the remaining layer. In the 4×4 antenna system, each of the two streams are multiplexed onto two antennas; the first stream is multiplexed onto the first and second antenna and the second stream onto the third and fourth antenna. The most recent versions of the 3G LTE specifications also include the 2×2 vertically encoded case, where a single code word is multiplexed on to two layers. In this scenario, decoding of the layers cannot be performed separately.

The transmission throughput is calculated as the nominal information transmission rate of information bits times $(1 - \mathrm{FER})$. A 5-MHz bandwidth was assumed in the simulations. The signal-to-noise ratio (SNR) represents E_s/N_0, where E_s is the symbol energy. Each SNR point includes transmission of 1000 frames. Perfect channel state information was assumed in the receiver. The typical urban (TU) channel [27] with BS azimuth spread of 2 degrees was applied. The normalized correlation between the spatial channels is about 0.8. There are six paths in the channel with the largest delay of 5000 ns. The base station (BS) antenna separation is 4 λ. Parameters of the used channel models are shown in Table II. In addition, a spatially uncorrelated channel was considered as well. The number of turbo decoder iterations in the simulations was 8.

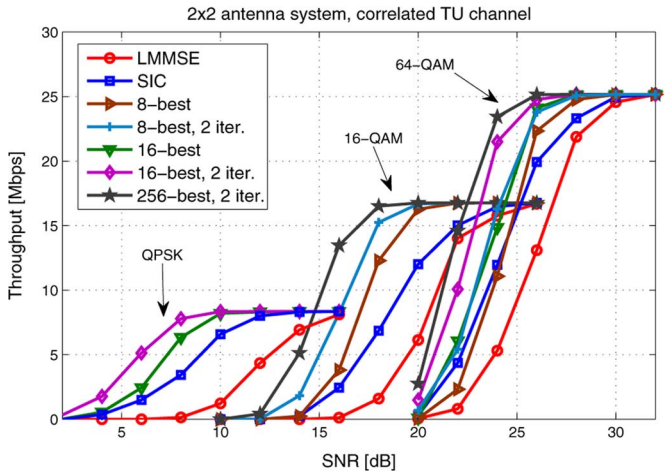

Fig. 5. Data transmission throughput versus SNR in a 2×2 H-BLAST system and correlated TU channel.

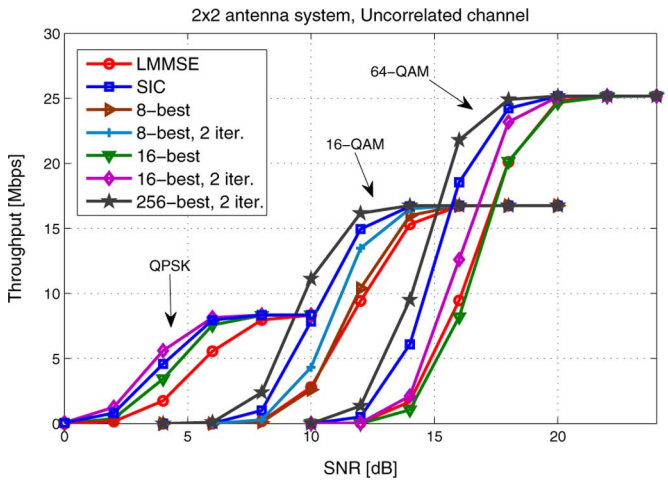

Fig. 6. Data transmission throughput versus SNR in a 2×2 H-BLAST system and uncorrelated channel.

A. 2×2 MIMO System

The throughput performances of the LMMSE, SIC and K-best detectors with 4-QAM, 16-QAM, and 64-QAM and two transmit and receive antennas is illustrated in Figs. 5–7. The highly correlated TU channel is applied in 5 and a spatially uncorrelated channel in 6; both figures assume horizontal encoding denoted as H-BLAST. A moderately correlated channel and vertical coding (denoted as V-BLAST) was assumed in Fig. 7. A real valued signal model was assumed in the K-best LSD and QRD of the channel matrix $\mathbf{H}$ with no sorting of the layers was used.

The results in Fig. 5 show that the K-best LSD outperforms the SIC receiver with all modulations under high correlation. Only the 8-best LSD with 64-QAM performs worse than the SIC in low SNRs. Using the turbo decoder outputs to update the LLRs in the LSD receiver improves the performance by roughly 1 dB compared to the LSD without any iterations. With 64-QAM, approximately the same performance is achieved with 8-best and two iterations as with 16-best without iterations. Performing interference cancellation improves the performance up to 4 dB compared to the LMMSE receiver. Turbo decoding for the bit LLRs is performed once both in the SIC receiver and the K-best receiver with no iterations. The iterative K-best LSD includes turbo decoding the bit LLRs twice.

The SIC receiver also outperforms the K-best LSD when the channel has no correlation as presented in Fig. 6. With highly correlated channels, the initial decisions in the SIC receiver are more likely to be incorrect which is found to lead to error propagation.

The SIC receiver improves the performance of the LMMSE receiver only very marginally in the vertically encoded system, as illustrated in Fig. 7. This is understandable and not surprising at all, because both layers have to be decoded before soft interference cancellation can be performed. Thus, the SIC receiver provides no benefit compared to the plain LMMSE receiver in the vertically encoded case, and it will be considered for the horizontally encoded case only in the sequel. The K-best LSD, on the other hand, performs similarly to the horizontally encoded case.

B. 4×4 MIMO System

The data transmission throughput versus SNR with four transmit and receive antennas is presented in Fig. 8. Two streams are encoded separately and the first stream is multiplexed onto the first two antennas and the second stream onto the third and fourth antenna [21]. Two iterations are performed with the SIC receiver. The symbols from the strongest layers are detected and decoded first and then cancelled from the remaining layers. The streams from the spatially multiplexed layers are separated only with the LMMSE equalizer in the SIC receiver. Interference cancellation is performed only between the two horizontally encoded streams. The correlation of the channels used in the simulations depends on the BS azimuth spreads of 2 degrees and 5 degrees, and it varied from 0.7 in Fig. 8(a) to 0.4 in Fig. 8(b). In the correlated TU channel, the K-best LSD outperforms the SIC and the LMMSE receivers. In the uncorrelated channel, the difference in performance is smaller and the SIC receiver outperforms the K-best LSD. With moderate correlation, the SIC performance is close to that of the K-best LSD. The performance of the SIC receiver is worse in the 4×4 antenna case than in the 2×2 case because cancellation is performed between the two streams and only LMMSE detection is used in the vertically encoded streams. This is due to the LTE encoding structure, which was described in the beginning of Section III.

C. Enhanced Tree Search and LLR Calculation

The impact of the enhanced tree search described in Section II-B-1) on the performance in a 2×2 64-QAM case is shown in Fig. 9. It can be seen that the performance degradation is minimal but the detection rate will be doubled. The new strategy is the most beneficial with high order modulations, when the nodes have several branches. When a lower order modulation is used, the performance degrades more with the new strategy.

The LLR calculation in the K-best LSD is simplified from (7) by leaving out the refinement part from (7). The impact of using the simplified LLR calculation is presented in Fig. 10.

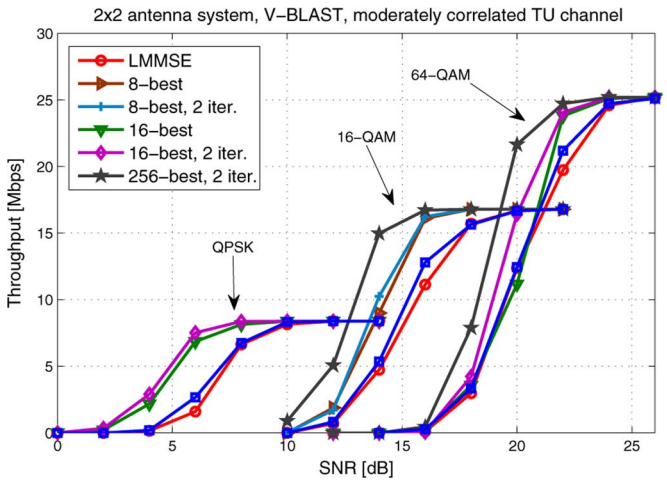

Fig. 7. Data transmission throughput versus SNR in a 2×2 V-BLAST system and moderately correlated channel.

The simplification has again only a small impact on the performance. Comparison of implementations done with the Catapult tool showed that the FPGA complexity is reduced approximately four times with the simplified LLR calculation. Also the SIC receiver is simplified from using soft demodulation for LLR calculation to using the approximate log-likelihood criterion. The symbol expectations are also calculated with (14).

IV. Implementation Comparisons

The theoretical complexity of the receivers with $M = N$ is presented in Table III, where the number of multiplication, addition, and comparison operations are specified. The memory is the number of bits used in each block. In the squared Givens rotations (SGR) and the Gram–Schmidt based QRD, the division and square root were approximated with additions and shifts [28]. The M^3 term in the SGR comes from matrix multiplications and in the QRD from multiple iterations of vector multiplications. The number of operations in the K-best algorithm depends on the list size K. If K is larger than $\sqrt{\Omega}^{(l-1)}$, it is used as K. In the first level l, the number of multiplications is $2\sqrt{\Omega}$ and additions $\sqrt{\Omega}$. The LLR calculation operations for the linear receivers depend on the modulation. The constant multiplications with a power of 2 were calculated as shifts. The number of multiplications is lower in the K-best LSD than in the SIC with 4×4 QPSK. The number of multiplications in the K-best algorithm increases with the list size and modulation. The modulation order does not have a major impact on the complexity with the SIC receiver. The impact of this can be seen later in the implementation results. The SIC receiver includes more multiplications than the K-best algorithm with 4×4 QPSK and the implementation gate count is also higher. With 64-QAM, the number of multiplications and gates is higher with the K-best.

Catapult C Synthesis tool [29] was used in the implementation of the receivers. It synthesizes algorithms written in ANSI C++ into high-performance, concurrent hardware. This single source methodology allows designers to pick the best architecture for a given performance/area/power specification while minimizing design errors and reducing the overall verification

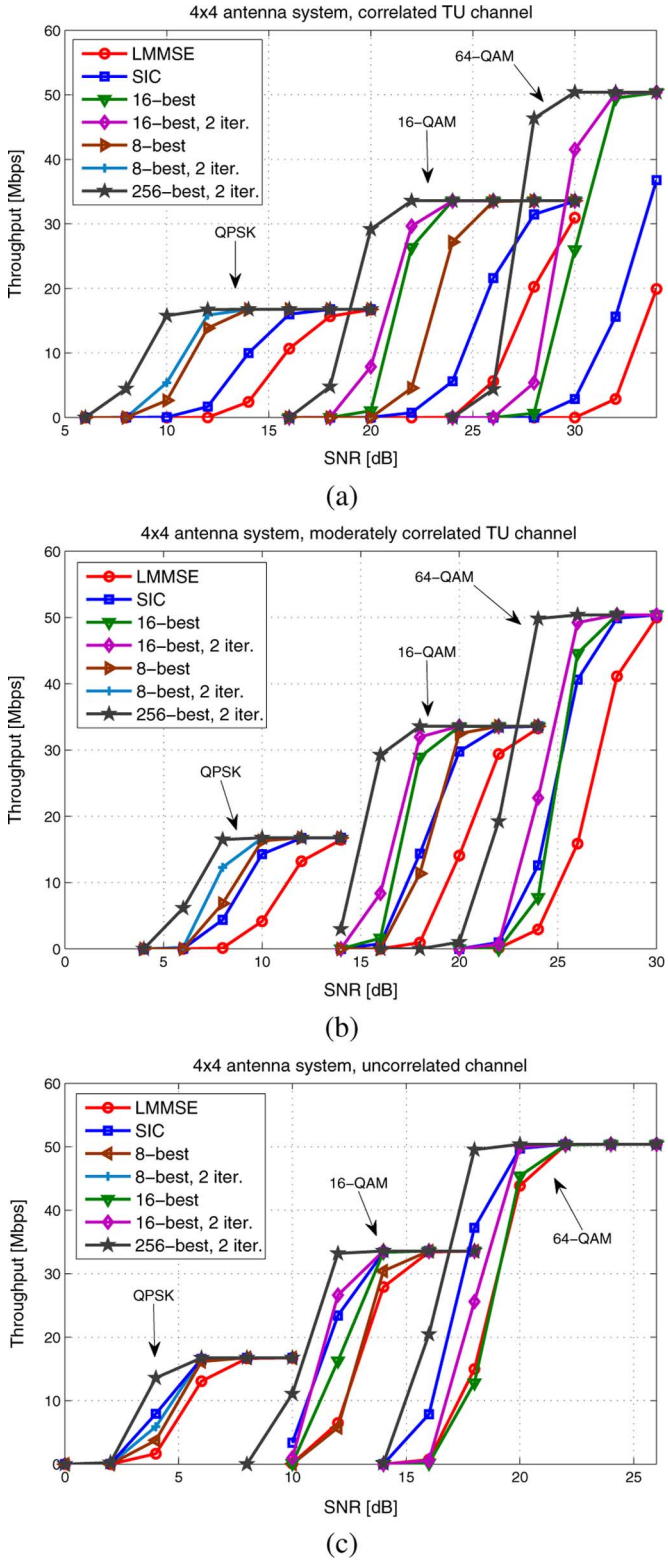

Fig. 8. Data transmission throughput versus SNR in a 4×4 system in (a) a highly correlated, (b) moderately correlated, and (c) uncorrelated channel.

burden. While the results may not always be as optimal as with hand-coded HDL, the tool allows experimenting with different architectures in a short amount of time and the comparison of different algorithms can be made, provided they are implemented with the same tool. The complexity results seem to be

TABLE III
THE THEORETICAL COMPLEXITY OF THE RECEIVERS AS NUMBERS OF ARITHMETIC OPERATIONS

Block	Multiplications	Additions	Comparisons	Memory
$(\mathbf{H}^{\mathrm{H}}\mathbf{H}+\sigma^2\mathbf{I}_M)$	$4M^3$	$(4M-2)M^2+M$		$16M^2$
SGR $(\mathbf{Q},\mathbf{R})$	$4M^3$+$4.5M^2$+$7.5M$-12	$4M^3+35M^2-45M-8$		$71M^2+18M$
$\mathbf{R}$ inverse	$\sum_{j=1}^{M-1} j^2$	$\sum_{j=1}^{M-1}(j^2-j)+40M$		$20M^2$
$\mathbf{R}^{-1}\mathbf{QH}$	$8M^3$	$(8M-4)M^2$		$32M^2$
Detection	$4M^2$	$3M^2-M$		$16M$
LLR (MMSE/SIC)	[2|8|16]M	$MQ/4$	[2|8|20]M	$8MQ$
Expectation calc.	$4M$		$M(18+Q/2)$	$8M$
SIC	$2M^2+4M$	$4M^2-M$		$80M$
QRD	$8M^3-M$	$8M^3-2M^2+93M$		$32M^2+40M$
Matrix-vector mult.	$4M^2$	$4M^2-2M$		$32M$
K-best LSD	$\sum_{l=2}^{2M} K\sqrt{\Omega}(l+1)$	$K\sum_{l=2}^{2M}\sqrt{\Omega}(l+1)$	$\sum_{l=2}^{2M} K^2\sqrt{\Omega}(l+1)$	$16K(M\sqrt{\Omega}+\sqrt{\Omega}+M+1)$
LLR (K-best)	K	$QM+32$	KQM	$5MQ$

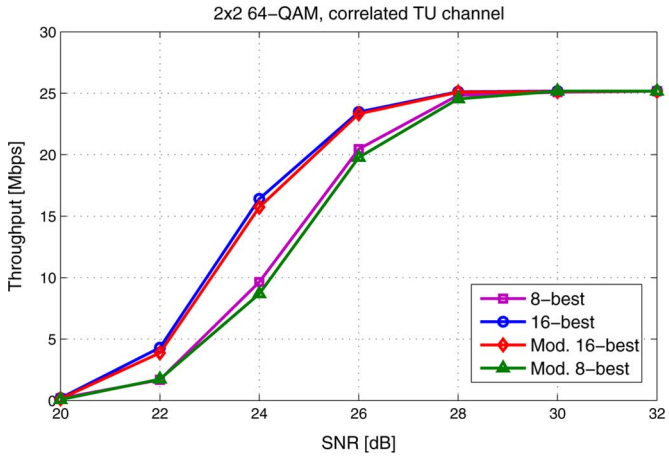

Fig. 9. Data transmission throughput versus SNR in a 2×2 system in a highly correlated channel with the modified tree search.

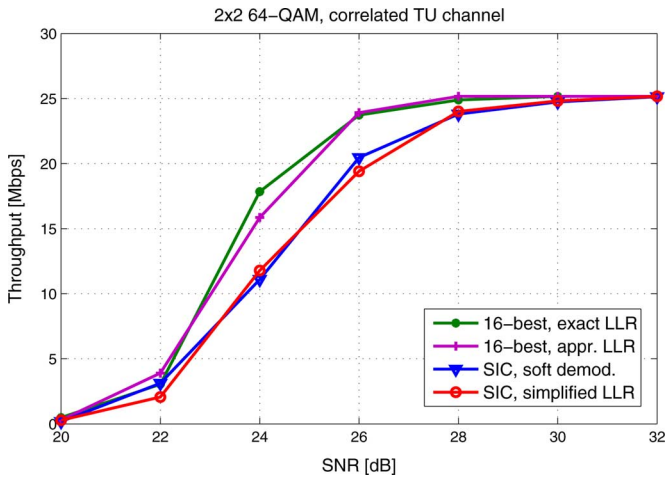

Fig. 10. Data transmission throughput versus SNR in a 2×2 system in a highly correlated channel with the simplified LLR calculation.

close to the hand-coded results with small designs. There can be more difference with large designs.

The FPGA complexity results are presented in slices, 18-kbit BRAM and dedicated DSP slices. The DSP slices include an 18×18-bit multiplier. The VHDL from Catapult C was synthesized to a Xilinx Virtex-4 FPGA with Mentor Graphics Precision Synthesis. The ASIC results are presented in gate

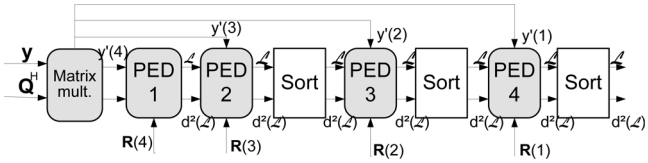

Fig. 11. The top-level architecture of the 2×2 K-best LSD.

equivalents (GE) and power consumption estimates. The Synopsys Design Compiler was used in synthesizing the VHDL along with the UMC 0.18 μm complementary metal oxide semiconductor (CMOS) technology. The Synopsys PrimePower was used for obtaining the statistical activity power estimates for the implementations.

A. K-Best LSD

The K-best LSD receiver includes the QRD block, the K-best LSD block and the LLR calculation block. The QR decomposition block is based on the QRD algorithm from [30]. Ordering of the channel matrix is not utilized in the architecture. The top level architecture of the K-best LSD for a 2×2 antenna system is shown in Fig. 11. The 4×4 antenna system LSD is based on the same architecture but four more PED calculation blocks and sorters are added to the design.

The K-best LSD architecture is modified from [20]. A 2×2 and a 4×4 antenna system with a real signal model [31] is assumed. The received signal vector $\mathbf{y}$ is multiplied with matrix $\mathbf{Q}$ in the matrix multiplication block. Matrix $\mathbf{R}$ is multiplied with the possible transmitted symbols after the QRD is performed, i.e., when the channel realization changes. Euclidean distances between the last symbol in vector $\mathbf{y}'$ and possible transmitted symbols are calculated in block PED1 in a 2×2 antenna system with $d(\mathbf{x}_4^2)=\|y_4'-r_{4,4}'\|^2$. The resulting lists of symbols and Euclidean distances are not sorted at the first stage. The distances are added to the Euclidean distances $d(\mathbf{x}_3^2)=\|y_3'-(r_{3,3}'+r_{3,4}')\|^2$ calculated in the PED2 block. The lists are sorted and K partial symbol vectors with the smallest Euclidean distances are kept. PED3 block calculates $d(\mathbf{x}_2^2)=\|y_2'-(r_{2,2}'+r_{2,3}'+r_{2,4}')\|^2$ which are added to the previous distance and sorted. The last PED block calculates the partial Euclidean distances $d(\mathbf{x}_1^2)=\|y_1'-(r_{1,1}'+r_{1,2}'+r_{1,3}'+r_{1,4}')\|^2$. After adding the previous distances to $d(\mathbf{x}_1^2)$, the lists are sorted

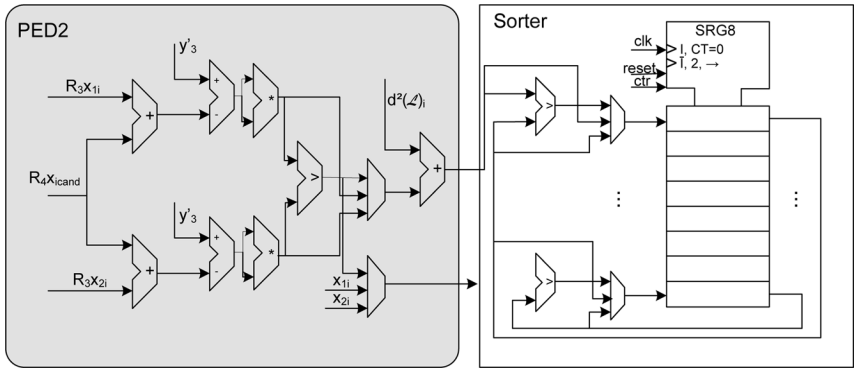

Fig. 12. Parallel PED calculation and sorting.

TABLE IV
THE 2×2 K-BEST LSD RECEIVER COMPLEXITY

Block	**Slices**	**DSPs**	**GE**	**mW**
QRD	1346	25	67 k	35.1
K**-best LSD**				
16-best, 4-QAM	913	28	54 k	79
8-best, 16-QAM	4172	15	110 k	120
8-best, 64-QAM	5712	22	124 k	261
16-best, 64-QAM	8818	16	166 k	246
LLR calculation, non-iterative/iterative				
4-QAM	1664/3485	5/5	27/34 k	32/51.8
16-QAM	746/1865	2/2	18/59 k	20/95.7
64-QAM, K=8	798/1666	2/2	25/51 k	29/66.7
64-QAM, K=16	1280/2241	2/2	36/46 k	38/68.7
Total, non-iterative/iterative				
4-QAM	3926/5747	58/58	148/155 k	146/166
16-QAM	6279/7398	42/42	197/236 k	175/251
64-QAM, K=8	7969/8837	49/49	219/241 k	326/364
64-QAM, K=16	11557/12518	43/43	267/277 k	319/350

TABLE V
THE 4×4 K-BEST LSD RECEIVER COMPLEXITY

Block	**Slices**	**DSPs**	**GE**	**mW**
QRD	39647	76	352 k	255
K**-best LSD**				
8-best, 4-QAM	9761	35	98 k	158
8-best, 16-QAM	14107	21	209 k	290
16-best, 16-QAM	27291	20	331 k	443
16-best, 64-QAM	16946	19	453 k	564
LLR calculation, non-iterative/iterative				
4-QAM	844/2958	2/2	18/57 k	20/96
16-QAM, K=8	776/3432	2/1	21/73 k	24/156
16-QAM, K=16	1326/6760	2/1	28/54 k	30/80
64-QAM	1299/6370	1/1	34/57 k	40/82
Total, non-iterative/iterative				
4-QAM	50252/52366	113/113	468/507 k	432/508
16-QAM, K=8	54530/57186	99/98	582/634 k	568/700
16-QAM, K=16	68264/73698	98/97	716/736 k	729/779
64-QAM	57892/62963	96/96	841/861 k	859/901

and the final K symbol vectors are demapped to bit vectors and their Euclidean distance is used in the LLR calculation.

The modified K-best LSD tree search was used in the implementation in the 64-QAM case. The architecture of the second stage parallel Euclidean distance calculation and insertion sorting is illustrated in Fig. 12. Two PEDs are calculated in parallel and the smallest one is added to the list.

The 2×2 K-best LSD receiver complexity is shown in Table IV and the 4×4 receiver complexity in Table V. Seven BRAMs are needed to store the results of the QRD in a 5-MHz bandwidth. In the iterative 2×2 64-QAM 16-best LSD, additional 9 BRAMs are needed to store the list and LLRs from the previous iteration. The clock frequency in the ASIC implementation is 140 MHz and in the FPGA implementation from 100 MHz to 94 MHz depending on the modulation.

The word lengths for the K-best LSD and LLR calculation are mainly 16 bits and computer simulations have been performed to confirm that there is no performance degradation [24]. The sorters are insertion sorters. The list size values of 16 and 8 are used in the implementation. The sorters have 16 or 8 registers in which the smallest Euclidean distances are kept during the sorting depending on the list size. A full list is used in the QPSK case and no sorting is required. This decreases the complexity of the detector.

The LLR calculation block was designed both for the iterative and noniterative receiver. The iterative LLR block was designed to have a low latency in order to perform additional global iterations quickly. The complexity of the block is therefore high. Using the decoder soft outputs in calculating the LLRs also adds to the complexity. If extra iterations are not needed, the LLR block can be scheduled to have the same latency as the K-best LSD and have a lower complexity.

B. Soft Interference Cancellation

The SIC receiver consists of a LMMSE detector, a LLR calculation block, a symbol expectation calculation block and an interference cancellation block as presented in Fig. 4. The top level architecture of the LMMSE detector for a 2×2 antenna system is presented in Fig. 13. The channel matrix $\mathbf{H}$ is first multiplied by its complex conjugate transpose and the noise variance σ^2 is added to the diagonal elements. The resulting 2×2 matrix $\mathbf{G}$ is positive definite and symmetric. This simplifies the matrix inversion, which is performed by dividing the elements with the determinant, switching the diagonals and negating the off-diagonal elements. The determinant is real valued and the off-diagonal elements are complex conjugates. Therefore, less operations are needed.

The architecture for the real part of the symbol expectation calculation in the 16-QAM case is presented in Fig. 14. The imaginary part is calculated in parallel in the same manner from

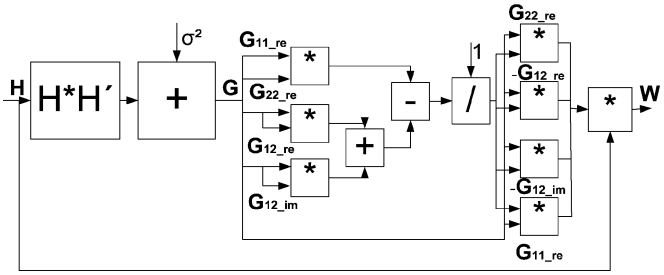

Fig. 13. The top level architecture of the 2 × 2 LMMSE detector.

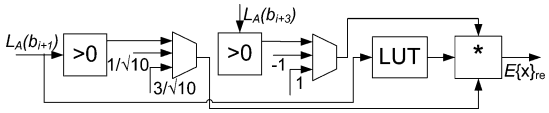

Fig. 14. The architecture of the symbol expectation calculation.

TABLE VI
THE 2 × 2 SYSTEM SIC RECEIVER COMPLEXITY

Block	Slices	DSPs	GE	mW
LMMSE	1481	39	48 k	40
LLR calculation, 4-QAM	34	10	13 k	14
LLR calculation, 16-QAM	59	17	18 k	19
LLR calculation, 64-QAM	434	18	27 k	21
Symbol. exp. calculation, 4-QAM	196	2	488	0.58
Symbol. exp. calculation, 16-QAM	258	6	1335	1.2
Symbol. exp. calculation, 64-QAM	232	10	3521	3.2
SIC	1407	53	17.5 k	22.3
Total, 4-QAM	3181	104	75 k	77
Total, 16-QAM	3268	115	85 k	83
Total, 64-QAM	3617	120	96 k	87

LLRs $L_A(b_i)$ and $L_A(b_{i+2})$ from the decoder. The lookup table (LUT) is used to find the $\tanh$ value.

The complexity of the SIC receiver for a 2 × 2 system is presented in Table VI. The word lengths were determined with computer simulations. In symbol expectation and LLR calculation blocks, the word lengths range from 6 to 16 bits. In the LMMSE block, word lengths up to 22 bits were used. In addition, four 18-kbit block RAMs are used to store the channel matrix $\mathbf{H}$ and the received symbol vector $\mathbf{y}$ and 1 BRAM is used in the interleaver. The LLR calculation block also includes detection, i.e., multiplying the received signal with the weight matrix $\mathbf{W}$. There are two ASIC implementations of the LMMSE block. The other one is used for the SIC receiver and has a lower latency and higher complexity. The clock frequency in the ASIC implementation is 100 MHz and from 105 MHz to 95 MHz in the FPGA implementation.

The complexity of the SIC receiver for a 4 × 4 system is presented in Table VII. The LMMSE detector is the most complex part of the receiver taking 95% of the slices and almost 80% of the gates. Performing a 4 × 4 matrix inversion in 4 clock cycles consumes a large portion of the resources. The LMMSE detector is based on the SGR [32]. The number of BRAMs needed to store the channel matrix, the weight matrix $\mathbf{W}$ and the received signal is 11. There are two LLR calculation blocks in the ASIC receiver, where the first one performs also detection and the other one is used to calculate only the LLRs in the second iteration. The decoder is not included in the total complexity.

TABLE VII
THE 4 × 4 SYSTEM SIC RECEIVER COMPLEXITY

Block	Slices	DSPs	GE	mW
LMMSE	29614	80	440 k	328
LLR calculation, 4-QAM	568	18	31 k	39
LLR calculation, 16-QAM	573	23	40 k	48
LLR calculation, 64-QAM	993	26	61 k	66
Symbol. exp. calculation, 4-QAM	47	4	664	0.56
Symbol. exp. calculation, 16-QAM	143	4	2346	1.2
Symbol. exp. calculation, 64-QAM	115	16	3146	2.2
SIC	687	29	59 k	72
Total, 4-QAM	30916	131	530 k	440
Total, 16-QAM	31017	136	540 k	449
Total, 64-QAM	31409	151	562 k	468

C. Latency Comparison

The processing latency of a receiver can be expressed as

$$D_{\mathrm{rec}} = D_{\mathrm{det}} + (D_{\mathrm{LLR}} + D_{\mathrm{dec}})N_{\mathrm{iter}} \tag{15}$$

where D_{det} is the latency of the detector, D_{LLR} is the latency of LLR calculation, D_{dec} is the latency of the decoder and N_{iter} is the number of iterations. If D_{LLR} and D_{dec} are small enough compared to D_{det}, LLR calculation and decoding can be performed simultaneously with detection and their latency does not have to be included in the total latency.

The detection rate of a receiver can be calculated as

$$\frac{1}{D_{\mathrm{rec}}} QN \tag{16}$$

where Q is the number of bits per symbol. The latencies presented in the following tables express the total latency of the block in clock cycles and the throughput period, i.e., the number of clock cycles in which each subcarrier is processed after the initial latency.

1) K-Best LSD: The latency estimations of the K-best LSD receiver are presented in Table VIII. The LSD is the timing bottleneck in the receiver. The QRD has the highest latency, but it is performed only once in the channel coherence time. The list $\mathcal{L}$ from the first iteration is used in calculating the LLRs in the second iteration. The second iteration can be performed while calculating the list for the next received symbol. Therefore, the detection rate of the iterative and noniterative K-best LSD is the same. The noniterative LLR block has the same latency as the K-best block. As the iterative 8-best LSD has the same performance as the noniterative 16-best LSD with 64-QAM, a higher goodput and lower complexity is achieved using the iterative 8-best LSD. In the ASIC implementation, the processing latency was set to 8 clock cycles. However, with the list size 16, scheduling was done to 16 clock cycles.

2) SIC: The latency estimations of the SIC receiver are presented in Table IX. The timing is further illustrated in Fig. 15, where the block latencies are presented in clock cycles. The throughput period is shown as the time after processing of the next subcarrier can begin. All the weight matrices in an OFDM symbol have to be calculated before a decision is made on which layer to detect first. The weight matrices are calculated when the channel realization changes, i.e., once in the channel coherence time. The latency of the LMMSE receiver does not depend on the modulation. The latency of turbo decoding is included in the

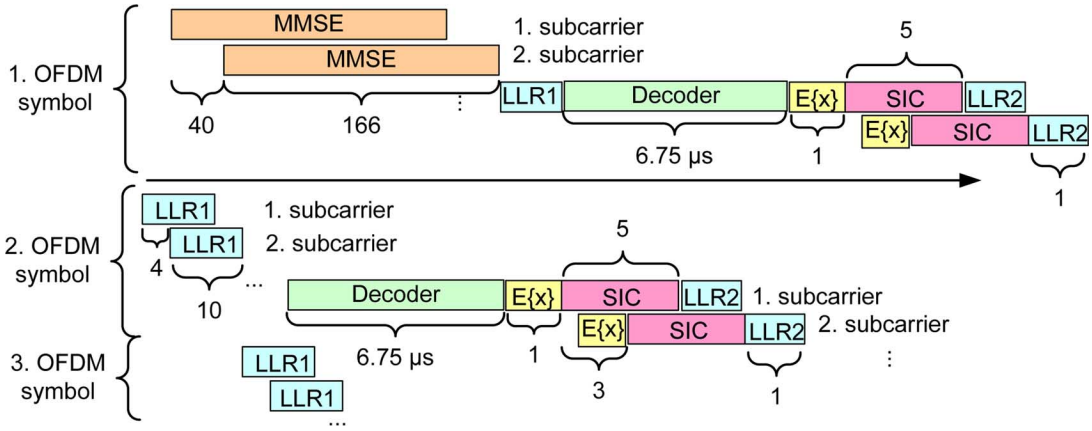

Fig. 15. The timing and latencies in the SIC receiver with 4×4 16-QAM.

TABLE VIII
LATENCY OF THE K-BEST LSD RECEIVER

	2×2		4×4	
Block	**FPGA**	**ASIC**	**FPGA**	**ASIC**
QRD	14 + 14	58 + 40	233 + 40	214 + 40
K-best, 4-QAM	37 + 4	20 + 8	153 + 12	98 + 8
K-best, 16-QAM	136 + 16	66 + 8	303 + 32	124 + 8
K-best, 64/16-QAM	143 + 16	75 + 8	433 + 48	172 + 16
K-best, 64-QAM	222+32	111+16	1084+128	203+16
LLR, 4-QAM	8 + 1	13 + 3	5 + 1	24 + 3
LLR, 16-QAM	5 + 6	24 + 3	8 + 2	19 + 3
LLR, 64/16-QAM	9 + 6	30 + 8	11 + 2	21 + 8
LLR, 64-QAM	15 + 12	41 + 16	13 + 4	26 + 16

TABLE IX
LATENCIES OF THE LMMSE AND SIC RECEIVERS

	2×2		4×4	
Block	**FPGA**	**ASIC**	**FPGA**	**ASIC**
LMMSE	28 + 4	60 + 40	51 + 4	166 + 40
LLR calc. 4-QAM	3 + 1	5 + 3	4 + 2	7 + 4
LLR calc. 16-QAM	6 + 1	7 + 3	8 + 2	10 + 4
LLR calc. 64-QAM	8 + 1	6 + 3	11 + 2	8 + 4
Symbol exp., 4-QAM	6 + 1	1 + 2	2 + 1	1 + 1
Symbol exp., 16-QAM	7 + 1	2 + 2	2 + 1	1 + 1
Symbol exp., 64-QAM	7 + 1	2 + 2	3 + 1	1 + 1
SIC	4 + 1	5 + 3	5 + 2	5 + 3

total latency estimate and it is calculated from the results given in [33], where the decoding rate is 711 Mb/s. The turbo decoder limits pipelining in the SIC receiver in a way that all the subcarriers have to be decoded before moving to the symbol expectation calculation. The LLR1 block includes detection and LLR calculation and it can start to process the next OFDM symbol while the second layer in the previous symbol is being calculated.

The LLR calculation block produces QN bit LLRs in the given latency period. Symbol expectations for a subcarrier are calculated in the given period. The latencies in the ASIC implementation were set to achieve the detection rates needed to process the data according LTE time frames in a 20-MHz bandwidth. 20 MHz is the maximum bandwidth in LTE, but lower bandwidths, such as the 5 MHz bandwidth used in the simulations, are also possible.

In the LTE specifications, a 0.5-ms slot has been allocated for 7 or 6 (depending on the length of the cyclic prefix length) OFDM symbols [21]. In the SIC receiver, seven OFDM symbols are processed in 0.46 ms when the MMSE weights are not calculated. Including the MMSE weight matrix calculation when the channel realization changes, averages the processing time to 0.5 ms. The slot time translates to detection rate with $7QNP/(0.5$ ms). The required detection rates in the 20-MHz bandwidth and a 2×2 antenna system are 68 Mb/s for QPSK, 136 Mb/s for 16-QAM, and 203 Mb/s for 64-QAM. The required rates are doubled in the 4×4 antenna case. The LMMSE receiver is fast enough to be used in all antenna and modulation cases. The SIC receiver does not achieve the required rates in the 4×4 case on FPGA but in other cases the requirements are met. The K-best LSD meets the requirements only in the 2×2 QPSK case on FPGA with the used technology. However, the K-best LSD could be used for a 5-MHz bandwidth. The ASIC implementations meet the requirements except with the 4×4 64-QAM and list size 16 in the 4×4 16-QAM case.

V. DISCUSSION

The theoretical complexities of the algorithms were presented. The complexity of the K-best algorithm is close to that of the SIC algorithm with low order modulations but the difference is greater with higher modulations. The implementation results in Section IV support the theoretical results in Table III: the receivers have similar complexities with low order modulations but the complexity of the K-best LSD increases with the modulation order. The LMMSE calculation was implemented as a direct matrix inversion in the 2×2 case which made the SIC less complex even with low order modulations.

The performance-complexity tradeoff of the ASIC implementations in a 2×2 16-QAM in a correlated channel is summarized in Table X and in the 4×4 16-QAM case in Table XI. The detection rates of the receivers are the same. Even though the detection rate of the LMMSE receiver is high, the performance degradation in terms of reliable transmission throughput is considerable in particular at the cell edge, where the available SNR is often low. Thus, the term goodput is defined to be the minimum of the hardware detection rate times the 1/2 code rate and the reliable transmission throughput (which, on the other hand, was defined in Section III as transmission rate of information bits over the 20-MHz bandwidth times

TABLE X
THE PERFORMANCE-COMPLEXITY TRADEOFF WITH 2 × 2 16-QAM AND DETECTION RATE OF 140 MB/S

Receiver	Complexity (GE)	Power mW	Goodput at 16 dB	Goodput at 20 dB
LMMSE	58 k	54	0.3 Mb/s	15.7 Mb/s
SIC	85 k	83	6.2 Mb/s	49.4 Mb/s
8-best	197 k	175	17.4 Mb/s	67.3 Mb/s
8-best, 2 iter.	236 k	251	32.4 Mb/s	69.8 Mb/s

TABLE XI
THE PERFORMANCE-COMPLEXITY TRADEOFF WITH 4 × 4 16-QAM AND DETECTION RATE OF 280 MB/S

Receiver	Complexity (GE)	Power mW	Goodput at 24 dB	Goodput at 28 dB
LMMSE	480 k	376	0.1 Mb/s	84.4 Mb/s
SIC	540 k	449	20.6 Mb/s	133.7 Mb/s
8-best	582 k	568	113.4 Mb/s	140 Mb/s
8-best, 2 iter.	634 k	700	128 Mb/s	140 Mb/s

$(1 - \mathrm{FER})$). The goodput now encapsulates performances of both the implementation and the transmission.

The LMMSE receiver would require almost 10 dB more transmit power in order to achieve the goodput of the K-best LSD but the complexity is much higher with the K-best LSD. The SIC receiver does not achieve the goodput of the K-best LSD but has a much lower complexity. In the 4×4 antenna case, the SIC and LMMSE receivers do not give much goodput at lower SNRs but all the receivers have a high goodput when the SNR is high enough. If the channel is less correlated, the receivers have a more similar performance and less transmit power is needed to achieve a high goodput. The SIC receiver produces the most bits per gate equivalent in the 2×2 antenna system but at the 4×4 system, the K-best LSD is the most efficient. A part of the performance degradation of the SIC receiver in the 4×4 antenna system is due to the encoding of the streams in LTE, which leads to interference cancellation being performed between two layer pairs and the two layer pairs being separated only by the LMMSE equalizer. The SIC receiver would still provide a higher goodput than the LMMSE receiver with a lower power consumption than the K-best LSD, thus offering a compromise between performance and complexity.

As a final illustration of the performance-complexity tradeoff, the required transmit power to satisfy the rate and quality requirements is considered in a simple example case. The power efficiency of the transmitter in transmit power/transmission rate in a 4×4 antenna system with a 20 MHz bandwidth is presented in Fig. 16. The needed transmit power was obtained from $L_F + N_R + \mathrm{SNR} + \mathrm{FM}$, where L_F is the free space path loss $20\log(4\pi d/\lambda)$, N_R is the receiver noise floor ($kTB+$ Receiver noise figure of 6 dB) and FM is a 30-dB fade margin (λ is the wavelength, d is the distance from the base station, k is Boltzmann's constant, T is the temperature [K] and B is the bandwidth). The SNR is the signal strength at the receiver required to achieve the maximum goodput. A simple path loss model without shadowing or reflections was chosen for simplicity. The required transmit power of the LMMSE receiver is at least twice of that of the K-best LSD. The transmit energy per bit grows with the modulation order and is the same with 64-QAM K-best

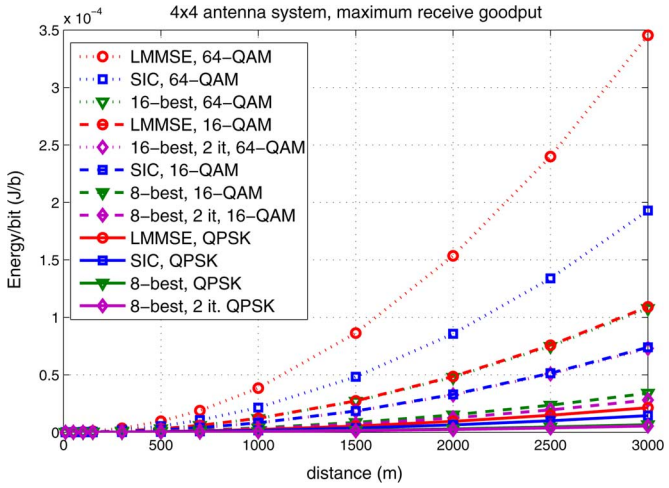

Fig. 16. The transmitter energy consumption per reliably transmitted bit versus the propagation distance.

LSD and 16-QAM LMMSE. The K-best LSD can receive data reliably from a higher distance than the SIC or LMMSE receiver with a fixed transmit power. With 4×4 64-QAM, the LMMSE receiver can receive data at only very short distances with a reasonable transmit power. Therefore, a more complex receiver is needed to receive data from also larger distances.

Comparison of both performance and implementation to literature can be difficult as the used channel models, methods and the implementation technologies may be different. Many of the implementations in the literature consider an uncoded system or an uncorrelated channel, where also simple receivers perform well, which can lead to different parameters in the implementation. Depth-first sphere detector implementations in the literature usually report an SNR dependent throughput which makes the implementation comparison more challenging. The hard-output l^2-norm K-best detectors in [19] have a lower complexity but were implemented with different list sizes and CMOS technology from our work. The complexity of the receiver increases by roughly 30% both in [19] and this work when the list size is doubled. However, the detection rate decreases almost five times in [19] but is only halved in our work. The soft output K-best implementation in [12] with a list size of 5 in a 4×4 16-QAM system has almost a three times lower throughput and half the complexity of our implementation with a list size 8. A soft output K-best detector is presented in [34]. It achieves a 50-Mb/s throughput with 4×4 64-QAM, list size 256 and a silicon area of 20 mm^2. The silicon area of our implementation is four times smaller with the same CMOS technology and the throughput is 210 Mb/s with a list size 16.

VI. CONCLUSION

The performances and implementation complexities of the LMMSE, SIC, noniterative and iterative K-best LSD receivers for MIMO–OFDM communications were compared. The emphasis was on LTE specific system parameters and latency requirements. The SIC receiver was shown to outperform the K-best LSD with horizontal encoding in channels with low spatial correlation, but the result is reversed in channels with significant spatial correlation; the SIC receiver is not practically

TABLE XII
THE RECEIVER WITH THE BEST GOODPUT (QAM CONSTELLATION Ω)

SNR	Corr.	Mod. corr.	Uncorr.
	2×2 system		
2 dB	it. 16-best (4)	it. 16-best (4)	it. 16-best (4)
10 dB	16-best (4)	16-best (4)	LMMSE (4)
15 dB	SIC (4)	SIC (16)	SIC (16)
20 dB	it. 8-best (16)	SIC (64)	SIC (64)
	4×4 system		
10 dB	it. 8-best (4)	8-best (4)	LMMSE (4)
15 dB	8-best (4)	LMMSE (4)	SIC (16)
20 dB	LMMSE (4)	8-best (16)	SIC (64)
25 dB	it. 8-best (16)	LMMSE (16)	LMMSE (64)

suitable for vertically encoded MIMO communications. Soft information feedback from the FEC decoder to the K-best LSD stage was also considered as a strategy to improve the performance. It provides up to 2-dB performance improvement. The choice of the receiver algorithm is emphasized when the number of antennas increases and the channel condition number is high. There the nonlinear ML or MAP based receivers clearly outperform the linear receivers, but the price is remarkably increased computational complexity.

The considered receivers were synthesized to a Xilinx FPGA to get a solid ground for implementation complexity comparison. A modification on the tree search of the K-best LSD was presented to simplify its implementation with no compromise in its error rate performance. Thus, it can achieve double detection rate compared to the original K-best algorithm. On the selected FPGA, the SIC receiver is fast enough to process the number of subcarriers defined in the LTE standard for 5-MHz bandwidth with all modulations and 2×2 and 4×4 antenna configurations. ASIC implementation results were also provided. The receivers were designed to have the same detection rate, which would be enough for the LTE 20-MHz bandwidth. The K-best LSD was found to be more than twice as complex as the SIC receiver in the 2×2 antenna case but in the 4×4 case the complexity difference was smaller. The latency of the SIC receiver does not depend on the used modulation and it can be used with higher order modulations. The latency of the K-best LSD increases with the modulation and the list size in both FPGA and ASIC implementations. The maximum detection rates in the ASIC implementations were 420 Mb/s with the SIC receiver and 280 Mb/s with the K-best LSD.

The receivers with the highest goodput and the lowest complexity on ASIC with correlated, moderately correlated and uncorrelated channels with a given SNR are presented in Table XII. It can be seen that the simpler LMMSE and SIC receivers can be used in the uncorrelated channel but in the correlated channel, the K-best LSD gives the best goodput. The receiver and the modulation order could be changed adaptively with the channel conditions and SNR in order to achieve the best possible goodput with the least amount of receive power.

Some open research problems still remain. The system we studied assumed that there is no channel state information at the transmitter. With full or partial transmitter channel state information, low mobility appropriate feedback schemes combined with transmitter precoding could change the conclusions and would be an interesting line of further work. Also adding channel estimation to the performance and complexity evaluation would be an interesting topic. One further promising topic would be the design and implementation of a reconfigurable overall architecture which would adaptively switch using a simple or a more complex detector depending on the transmission requirements, available SNR, channel properties, etc. Some preliminary results for the study of receivers for adaptive modulation and coding can be found in [35].

ACKNOWLEDGMENT

The authors would like to thank Mentor Graphics for the possibility to evaluate Catapult C Synthesis tool and M. Myllylä and J. Ylioinas for their helpful comments.

REFERENCES

[1] H. Boelcskei, "MIMO-OFDM wireless systems: Basics, perspectives, and challenges," *IEEE Trans. Commun.*, vol. 13, no. 4, pp. 31–37, Aug. 2006.

[2] H. Artes, D. Seethaler, and F. Hlawarsch, "Efficient detection algorithms for MIMO channels: A geometrical approach to approximate ML detection," *IEEE Trans. Signal Process.*, vol. 51, no. 11, pp. 2808–2820, Nov. 2003.

[3] G. J. Foschini and M. J. Gans, "On limits of wireless communications in a fading environment when using multiple antennas," in *Wireless Pers. Commun.*. : Kluwer, 1998, vol. 6, pp. 311–335.

[4] P. W. Wolniansky, G. J. Foschini, G. D. Golden, and R. A. Valenzuela, "V-BLAST: An architecture for realizing very high data rates over the rich-scattering wireless channel," in *Proc. Int. Symp. Signals, Systems, Electronics (ISSSE)*, Pisa, Italy, Sept. 29–Oct. 2 1998, pp. 295–300.

[5] G. D. Golden, C. J. Foschini, R. A. Valenzuela, and P. W. Wolniansky, "Detection algorithm and initial laboratory results using V-BLAST space-time communication architecture," *IEE Electron. Lett.*, vol. 35, no. 1, pp. 14–16, Jan. 1999.

[6] X. Wautelet, A. Dejonghe, and L. Vandendorpe, "MMSE-based fractional turbo receiver for space-time BICM over frequency-selective MIMO fading channels," *IEEE Trans. Signal Process.*, vol. 52, no. 6, pp. 1804–1809, Jun. 2004.

[7] M. Sellathurai and S. Haykin, "TURBO-BLAST for wireless communications: Theory and experiments," *IEEE Trans. Signal Process.*, vol. 50, no. 10, pp. 2538–2546, Oct. 2002.

[8] M. O. Damen, H. El Gamal, and G. Caire, "On maximum–likelihood detection and the search for the closest lattice point," *IEEE Trans. Inf. Theory*, vol. 49, no. 10, pp. 2389–2402, Oct. 2003.

[9] U. Fincke and M. Pohst, "Improved methods for calculating vectors of short length in a lattice, including a complexity analysis," *Math. Comput.*, vol. 44, no. 5, pp. 463–471, May 1985.

[10] B. Hochwald and S. ten Brink, "Achieving near-capacity on a multiple-antenna channel," *IEEE Trans. Commun.*, vol. 51, no. 3, pp. 389–399, Mar. 2003.

[11] K. Wong, C. Tsui, R. K. Cheng, and W. Mow, "A VLSI architecture of a K-best lattice decoding algorithm for MIMO channels," in *Proc. IEEE Int. Symp. Circuits Systems*, Scottsdale, AZ, May 26–29, 2002, vol. 3, pp. 273–276.

[12] Z. Guo and P. Nilsson, "Algorithm and implementation of the K-best sphere decoding for MIMO detection," *IEEE J. Sel. Areas Commun.*, vol. 24, no. 3, pp. 491–503, Mar. 2006.

[13] C. Studer, A. Burg, and H. Bolcskei, "Soft-output sphere decoding: Algorithms and VLSI implementation," *IEEE J. Sel. Areas Commun.*, vol. 26, no. 2, pp. 290–300, Feb. 2008.

[14] M. Myllylä, M. Juntti, and J. R. Cavallaro, "Architecture design and implementation of the increasing radius—List sphere detector algorithm," in *Proc. IEEE Int. Conf. Acoust., Speech, Signal Processing*, Taipei, Taiwan, Apr. 2009, pp. 553–556.

[15] P. Bhagawat, R. Dash, and G. Choi, "Systolic like soft-detection architecture for 4×4 64-QAM MIMO system," in *Proc. Design, Automation Test in Eur. Conf. Exhibit.*, Nice, France, Apr. 2009, pp. 870–873.

[16] S. Mondal, A. M. Eltawil, and K. N. Salama, "Architectural optimizations for low-power K-best MIMO decoders," *IEEE Trans. Veh. Technol.*, vol. 58, no. 7, pp. 3145–3153, Sep. 2009.

[17] J. Antikainen, P. Salmela, O. Silvén, M. Juntti, J. Takala, and M. Myllylä, "Fine-grained application-specific instruction set processor design for the K-best list sphere detector algorithm," in *Proc. Int. Symp. Systems, Architectures, Modeling, Simulation (SAMOS)*, Samos, Greece, Jul. 21–24, 2008, pp. 108–115.

[18] K. Amiri, J. R. Cavallaro, C. Dick, and R. M. Rao, "A high throughput configurable SDR detector for multi-user MIMO wireless systems," *J. Signal Process. Syst.*, Apr. 2009.
[19] A. Burg, "VLSI Circuits for MIMO Communication Systems," Ph.D. dissertation, ETH, Zurich, Switzerland, 2006.
[20] J. Ketonen and M. Juntti, "SIC and K-best LSD receiver implementation for a MIMO-OFDM system," presented at the Eur. Signal Process. Conf., Lausanne, Switzerland, Aug. 25–29, 2008.
[21] Third Generation Partnership Project (3GPP); Technical Specification Group Radio Access Network, "Evolved Universal Terrestrial Radio Access E-UTRA; Physical channels and modulation TS 36.211 (Version 8.5.0)," Tech. Rep., 2008.
[22] M. Myllylä, J. Antikainen, M. Juntti, and J. Cavallaro, "The effect of LLR clipping to the complexity of list sphere detector algorithms," in *Proc. Annu. Asilomar Conf. Signals, Syst., Comp.*, Pacific Grove, CA, Nov. 4–7, 2007, pp. 1559–1563.
[23] J. Ylioinas and M. Juntti, "Iterative joint detection, decoding, and channel estimation in turbo coded MIMO-OFDM," *IEEE Trans. Veh. Technol.*, vol. 58, no. 4, pp. 1784–1796, May 2009.
[24] J. Ketonen, M. Myllylä, M. Juntti, and J. R. Cavallaro, "ASIC implementation comparison of SIC and LSD receiver for MIMO-OFDM," presented at the Annu. Asilomar Conf. Signals, Syst., Comp., Pacific Grove, CA, Oct. 25–29, 2008.
[25] I. Collings, M. Butler, and M. McKay, "Low complexity receiver design for MIMO bit-interleaved coded modulation," in *Proc. IEEE Int. Symp. Spread Spectrum Techniques and Applications*, Sydney, Australia, Aug. 30–Sep. 2 2004, pp. 1993–1997.
[26] M. Tüchler, A. C. Singer, and R. Koetter, "Minimum mean squared error equalisation using *a priori* information," *IEEE Trans. Signal Process.*, vol. 50, no. 3, pp. 673–683, Mar. 2002.
[27] Third Generation Partnership Project (3GPP); Technical Specification Group Radio Access Network, 3rd Generation Partnership Project (3GPP), "Radio Transmission and Reception (3G TS 45.005 Version 5.4.0 (Release 5))," Tech. Rep., 2002.
[28] B. Parhami, *Computer Arithmetic: Algorithms and Hardware Designs*. New York: Oxford Univ. Press, 2000.
[29] Mentor Graphics Datasheet, "Catapult synthesis," Tech. Rep., 2008 [Online]. Available: http://www.mentor.com/products/esl/high_level_synthesis/catapult_synthesis/index.cfm
[30] D. Wübben, R. Böhnke, V. Kühn, and K. Kammeyer, "MMSE extension of V-BLAST based on sorted QR decomposition," in *Proc. IEEE Veh. Technol. Conf.*, Orlando, FL, Oct. 6–9, 2003, vol. 1, pp. 508–512.
[31] M. Myllylä, M. Juntti, and J. R. Cavallaro, "Implementation aspects of list sphere detector algorithms," in *Proc. IEEE Global Telecommun. Conf.*, Washington, DC, Nov. 26–30, 2007, pp. 3915–3920.
[32] R. Döhler, "Squared givens rotation," *IMA J. Numer. Anal.*, vol. 11, pp. 1–5, 1991.
[33] Y. Sun, Y. Zhu, M. Goel, and J. Cavallaro, "Configurable and scalable high throughput turbo decoder architecture for multiple 4G wireless standards," in *Proc. IEEE Int. Conf. Application-Specific Systems, Architectures Processors (ASAP)*, Leuven, Belgium, Jul. 2–4, 2008, pp. 209–214.
[34] S. Chen, T. Zhang, and Y. Xin, "Breadth-first tree search MIMO signal detector design and VLSI implementation," in *Proc. IEEE Military Commun. Conf.*, Atlantic City, NJ, Oct. 17–20, 2005, pp. 1470–1476.
[35] J. Ketonen, M. Juntti, and J. R. Cavallaro, "Receiver implementation for MIMO-OFDM with AMC and precoding," presented at the Annu. Asilomar Conf. Signals, Syst., Comput., Pacific Grove, CA, Nov. 1–4, 2009.

Johanna Ketonen (S'07) received the M.Sc. (Tech.) degree in electrical and information engineering from the University of Oulu, Oulu, Finland, in 2007. She is currently working toward the Dr.Sc. (Tech.) at the Centre for Wireless Communications, University of Oulu, Oulu, Finland.

Her main research interests are in the implementation oriented study of receiver algorithms for MIMO-OFDM systems.

Markku Juntti (S'93–M'98–SM'04) received the M.Sc. (Tech.) and Dr.Sc. (Tech.) degrees in electrical engineering from University of Oulu, Oulu, Finland, in 1993 and 1997, respectively.

He was with University of Oulu from 1992 to 1998. During the academic year 1994–1995, he was a Visiting Scholar at Rice University, Houston, TX. From 1999 to 2000, he was a Senior Specialist with Nokia Networks. He has been a Professor of Telecommunications in the Department of Electrical and Information Engineering and Centre for Wireless Communications (CWC) at the University of Oulu since 2000. His research interests include signal processing for wireless networks as well as communication and information theory. He is an author or coauthor in some 200 papers published in international journals and conference records as well as in the book *WCDMA for UMTS* (Wiley, 2000). He is also an Adjunct Professor at the Department of Electrical and Computer Engineering, Rice University, Houston, TX.

Dr. Juntti is an Editor of the IEEE TRANSACTIONS ON COMMUNICATIONS and was an Associate Editor for the IEEE TRANSACTIONS ON VEHICULAR TECHNOLOGY from 2002 to 2008. He was Secretary of IEEE Communication Society Finland Chapter from 1996 to 1997 and the Chairman from 2000 to 2001. He has been Secretary of the Technical Program Committee (TPC) of the 2001 IEEE International Conference on Communications (ICC'01) and the Co-Chair of the Technical Program Committee of 2004 Nordic Radio Symposium and 2006 IEEE International Symposium on Personal, Indoor and Mobile Radio Communications (PIMRC 2006).

Joseph R. Cavallaro (S'78–M'82–SM'05) received the B.S. degree from the University of Pennsylvania, Philadelphia, in 1981, the M.S. degree from Princeton University, Princeton, NJ, in 1982, and the Ph.D. degree from Cornell University, Ithaca, NY, in 1988, all in electrical engineering.

From 1981 to 1983, he was with AT&T Bell Laboratories, Holmdel, NJ. In 1988, he joined the faculty of Rice University, Houston, TX, where he is currently a Professor of electrical and computer engineering. His research interests include computer arithmetic, VLSI design and microlithography, and DSP and VLSI architectures for applications in wireless communications. During the 1996–1997 academic year, he served at the National Science Foundation as Director of the Prototyping Tools and Methodology Program. He was a Nokia Foundation Fellow and a Visiting Professor at the University of Oulu, Finland, in 2005 and continues his affiliation there as an Adjunct Professor. He is currently the Associate Director of the Center for Multimedia Communication at Rice University.

Dr. Cavallaro was Co-Chair of the 2004 Signal Processing for Communications Symposium at the IEEE Global Communications Conference and General Co-Chair of the 2004 IEEE Fifteenth International Conference on Application-Specific Systems, Architectures and Processors (ASAP).